Environmental Science & Technology

pubs.acs.org/est

Article

Temporal Dynamics of Antibiotic Resistome in the Plastisphere during Microbial Colonization

Kai Yang, Qing-Lin Chen, Mo-Lian Chen, Hong-Zhe Li, Hu Liao, Qiang Pu, Yong-Guan Zhu, and Li Cui*

Cite This: *Environ. Sci. Technol.* 2020, 54, 11322−11332

Read Online

ACCESS | Metrics & More | Article Recommendations | Supporting Information

ABSTRACT: The increasing and simultaneous pollution of plastic debris and antibiotic resistance in aquatic environments makes plastisphere a great health concern. However, the development process of antibiotic resistome in the plastisphere is largely unknown, impeding risk assessment associated with plastics. Here, we profiled the temporal dynamics of antibiotic resistance genes (ARGs), mobile genetic elements (MGEs), and microbial composition in the plastisphere from initial microbial colonization to biofilm formation in urban water. A total of 82 ARGs, 12 MGEs, and 63 bacterial pathogens were detected in the plastisphere and categorized as the pioneering, intermediate, and persistent ones. The high number of five MGEs and six ARGs persistently detected in the whole microbial colonization process was regarded as a major concern because of their potential role in disseminating antibiotic resistance. In addition to genomic analysis, D_2O-labeled single-cell Raman spectroscopy was employed to interrogate the ecophysiology of plastisphere in a culture-independent way and demonstrated that the plastisphere was inherently more tolerant to antibiotics than bacterioplankton. Finally, by combining persistent MGEs, intensified colonization of pathogenic bacteria, increased tolerance to antibiotic, and potential trophic transfer into a holistic risk analysis, the plastisphere was indicated to constitute a hot spot to acquire and spread antibiotic resistance and impose a long-term risk to ecosystems and human health. These findings provide important insights into the antibiotic resistome and ecological risk of the plastisphere and highlight the necessity for comprehensive surveillance of plastisphere.

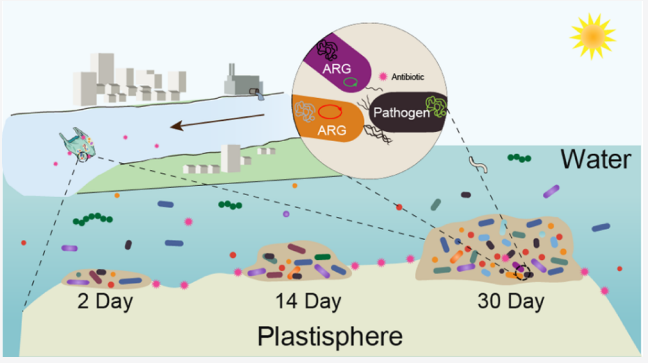

INTRODUCTION

Plastics have been used in a wide variety of products because of their malleability and durability properties and low cost. However, the intense consumption and disposal of plastic products are leading to rapid accumulation of plastic debris in the environment.[1] Plastic debris has become omnipresent in aquatic ecosystems, such as seas,[2] urban rivers,[3] coastal waters,[4] lakes,[5] and reservoirs.[6] In addition, plastic debris surfaces can be colonized by microorganisms to form biofilms, the so-called "plastisphere".[7,8] It was estimated that the microbial biomass harbored on plastics could even exceed 6% of its total mass,[9] and certain microbial community members could be harmful pathogens.[8,10]

With the rapidly increasing occurrence and dissemination of antibiotic resistance in the environment, an aquatic ecosystem has become enriched with antibiotic-resistant bacteria (ARB) and antibiotic resistance genes (ARGs).[11] Antibiotic resistance enables bacteria to circumvent antibiotic treatment by producing enzymes to degrade antibiotics, preventing antibiotics from reaching its target *via* an efflux pump or modifying the target. Its prevalence, especially in clinically relevant pathogens, has greatly compromised the antibiotic therapy for bacterial infections and poses a global threat to health.[12] Plastics coming into contact with these ecosystems are inevitably contaminated with antibiotic resistance. It has been estimated that over 10,000 tons of plastics are floating in the open ocean.[13] Recent investigations have revealed that plastics are great reservoirs of ARB and ARGs in the marine environment.[14,15] Additionally, as a hydrophobic substrate, plastics can readily accumulate organic and inorganic pollutants in the environment, such as antibiotics,[16] heavy metals,[17] pesticides,[18] and other persistent organic pollutants.[19,20] These chemicals were expected to drive the selection/co-selection of antibiotic resistance,[21] thus making plastics a specific and even favorable niche for the dissemination of antibiotic resistance.[22,23] Increased rate of ARG transfer in the plastisphere than their free-living

Received: June 30, 2020
Revised: August 18, 2020
Accepted: August 19, 2020
Published: August 19, 2020

https://dx.doi.org/10.1021/acs.est.0c04292
Environ. Sci. Technol. 2020, 54, 11322−11332

counterparts was demonstrated.[24] Furthermore, with the transportation and trophic transfer of plastics harboring antibiotic resistance, concerns regarding their negative impact on water, food supply, and human health are rising.[7,23,25,26] Understanding the development process of antibiotic resistome in the plastisphere is of great importance for their risk evaluation.

Currently, investigations on antibiotic resistome in the plastisphere were largely based on field samplings.[14,15,27,28] These studies revealed that plastics in an aquaculture system harbored diverse ARGs and ARB.[28] However, little is known about the occurrence and temporal variations of antibiotic resistome from microbial colonization to biofilm formation on plastic surfaces, such as the pioneering, intermediate, and persistent antibiotic resistance in plastisphere. Only a few works targeted the temporal dynamics of colonization process in the plastisphere and rather focused on the taxonomic composition of the microbial community.[29] Temporal dynamics of antibiotic resistome in the plastisphere are still largely unknown, impeding the assessment of ecological risks of plastics. In addition to the genomic level, association with plastics has the potential to affect bacterial resistance at physiological levels, such as the phenotypic resistance or tolerance to antibiotic treatment. In the biofilm structure of plastisphere, microbes aggregate and embed in self-secreted extracellular polymeric substances (EPS).[7,8,30] This structure enables microbes on plastics to be potentially more tolerant to antibiotics than planktonic cells and survive a long time during transportation, raising their risk of spreading antibiotic resistance and causing disease.[7] However, a quantitative evaluation of the physiological response of bacteria on plastics is still lacking.

In this work, we established an exposure time-series experiment in which polyethylene plastic debris was exposed to surface water from Xinglin Bay at Xiamen for 30 days, a rapidly urbanizing aquatic ecosystem flowing through residential and business areas and receiving a lot of impact of anthropogenic activities such as land runoff and wastewater pipe. To achieve an integrated profile of ARGs and mobile genetic elements (MGEs) in the plastisphere, a high-throughput quantitative polymerase chain reaction (qPCR) with up to 384 validated primer sets targeting almost all major classes of ARGs and 49 MGE marker genes was used to analyze the temporal dynamics of the diversity and abundance of antibiotic resistome in the plastisphere and the surrounding water. Furthermore, single-cell Raman spectroscopy combined with D_2O-labeling was employed to compare the antibiotic tolerance of microbes in the plastisphere and the planktonic state. We aim to achieve (1) an in-depth understanding of the occurrence and temporal variation of antibiotic resistome during microbial colonization and biofilm development on plastic surfaces, especially to identify the initial, intermediate, and persistent resistome and their link with the colonized microbial community and (2) an understanding of the potential risk by holistic analysis of ARGs, MGEs, pathogenic bacteria, and phenotypic antibiotic tolerance in the plastisphere at both genomic and physiological levels. These findings will provide important insights into the antibiotic resistome in the plastisphere and its potential risks to the aquatic ecosystem and human health.

MATERIALS AND METHODS

Materials and Experimental Setup. *Plastic Films.* High-density polyethylene food bags (Cleanwrap Co., Ltd.) were cut with sterilized scissors to produce 3 cm × 3 cm plastic sheets. These plastic sheets were treated with 70% ethanol for 30 min and rinsed three times with sterile water for disinfection.

Source Water. The source microbial community was obtained from the surface water of Xinglin Bay, Xiamen, China (24°36′ N, 118°03′ E) in March 2019. The water was prefiltered with 10 and 3 μm microfiltration membranes (Merck Millipore Ltd., Ireland) in tandem to remove big particles and potential grazers. The basic physiochemical parameters of source water are listed in Table S1.

Biofilm Reactor Setup. A CDC biofilm reactor (BioSurface Technologies, MT, USA) was used to grow biofilms on the surface of plastic membranes. The plastic membranes were mounted on the rod of a CDC biofilm reactor. The source water was flowed through the reactor at 4 mL min^{-1} by a peristaltic pump and stirred at 130 rpm for 30 days at room temperature (ca. 30 °C) by a magnetic stirrer. After different incubation times (0, 2, 14, and 30 days), the plastic sheets were taken out from the reactor and stored at −20 °C for further analysis.

Biofilm Quantification. During microbial colonization, biofilm quantification including the biofilm assay, buoyancy test, contact angle measurement, and scanning electron microscopy (SEM) was done, which are described in detail in the Supporting Information.

DNA Extraction. DNA was extracted from plastic sheets and water samples using the FastDNA Spin Kit for Soil (MP Biomedicals, Santa Ana, USA) according to the manufacturer's guidelines. In total, 600 mL water samples and 4 pieces of plastic sheets (with a total surface area of 18 cm^2; from different sampling times (0, 2, 14, and 30 days) were used for DNA extraction in triplicate. Water samples were filtered through sterile 0.22 μm polycarbonate filters (Merck Millipore Ltd., Ireland), which were then subjected to DNA extraction. Before DNA extraction, the plastic sheets and polycarbonate filters were cut into pieces using sterile scissors. DNA retrieved from the plastic sheets was eluted in 60 μL DES buffer (QIAGEN, Hilden, Germany). The concentration of DNA was quantified using a QuantiFluor dsDNA assay kit (Promega, WI, USA) with a Qubit 3.0 Fluorometer (Thermo Fisher Scientific Inc., Waltham, USA). Finally, the DNA extracts of all samples were stored at −20 °C until further analysis.

High-Throughput qPCR. To characterize the profiles of ARGs and MGEs, HT-qPCR was performed using a SmartChip Real-Time PCR System (WaferGen Inc., Fremont, CA, USA) in triplicate per sample. The SmartChip nanowell platform can be used for large-scale genotyping studies by processing 5184 qPCR reactions in parallel. A total of 384 primer pairs were used to target 327 ARGs, 7 taxonomic genes, 49 MGE marker genes including 11 transposase genes, 11 plasmids, 3 integrase genes, 24 insertional sequences, and 16S rRNA genes. HT-qPCR mixtures consisted of the DNA template, primer, LightCycler 480 SYBR Green I Master (Roche Applied Sciences, Indianapolis, IN), nuclease-free PCR-grade water, and bovine serum albumin (New England Biolaboratories, Beverly, MA). The mixtures were dispensed into a 5184-well chip using a SmartChip MultiSample NanoDispenser, followed by real-time qPCR using a SmartChip Cycler. The thermal cycle of HT-qPCR consisted

https://dx.doi.org/10.1021/acs.est.0c04292
Environ. Sci. Technol. 2020, 54, 11322−11332

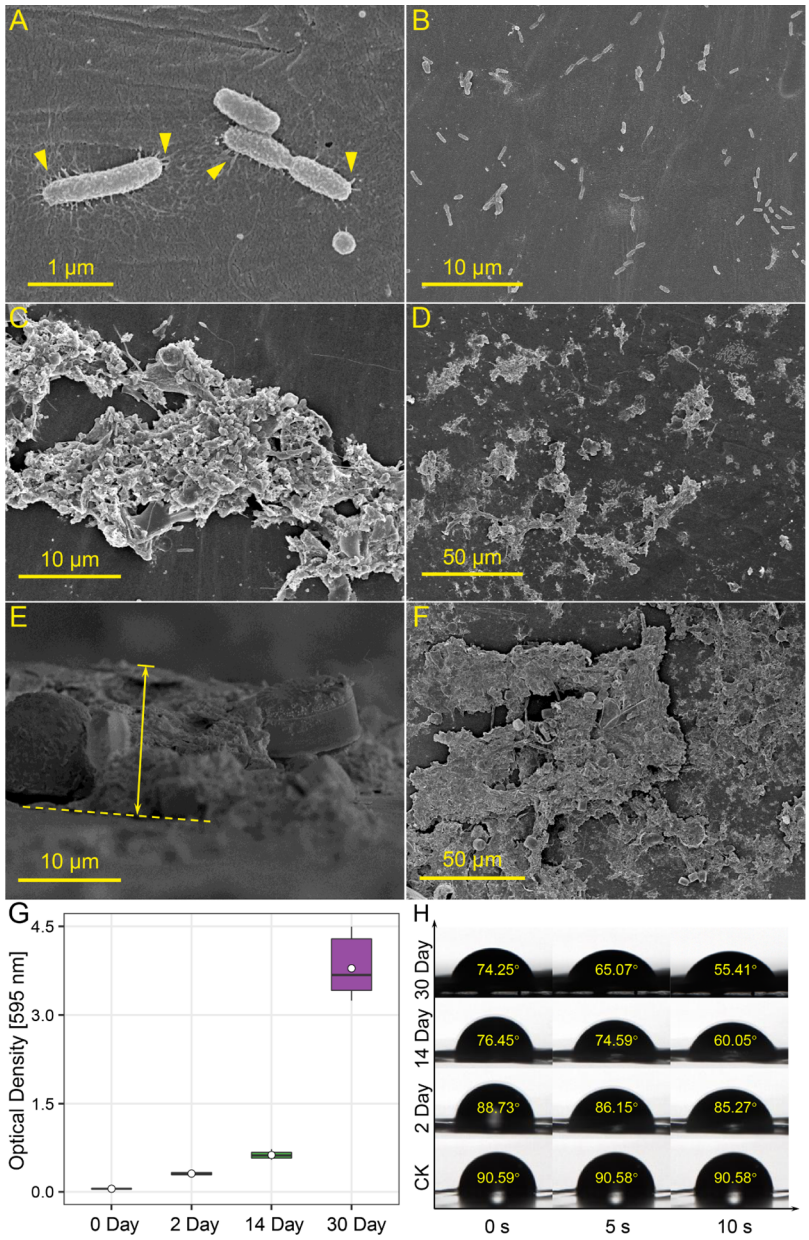

Figure 1. Physicochemical properties of plastic surfaces during microbial colonization on plastic debris. SEM images of microbial colonization on plastics after 2 days (A,B) and 14 days (C,D) of incubation. Cell appendages attached to plastic surfaces were shown as arrow heads in (A). (E) Cross-sectional and (F) surface views of SEM images of microbial colonization after 30 days of incubation. (G) Microbial biomass on plastics measured as the optical density at 595 nm. (H) Contact angle (θ_w) of biofilms on the plastic surface.

of 95 °C for 10 min followed by 40 cycles of denaturation at 95 °C for 30 s and annealing at 60 °C for 30 s. Nontemplate negative controls were performed with every primer set. Melting curve analyses were automatically generated by WaferGen software. The qPCR results were analyzed using SmartChip qPCR software (2.7.0.1 version), and wells with multiple melting peak and amplification efficiencies beyond the range (1.8−2.2) were discarded. A threshold cycle (C_t) of 31 was used as the detection limit, and only samples with all three technical replicates being amplified were regarded as positive and used in further data analysis. Relative copy numbers were calculated as follows: relative gene copy number = $10^{(31-C_t)(10/3)}$, where C_t equals the threshold cycle.

Illumina Sequencing and Data Processing. To characterize the taxonomic profiles of bacterial communities (BCs), the V4−V5 hypervariable region of the 16S rRNA gene was amplified with primer pairs (515 F: 5′-GTGCCAGCMGCCGCGG-3′ and 907 R: 5′-CCGTCAATCMTTTRAGTTT-3′).[31] Detailed information on the library preparation and data processing is provided in the Supporting Information. For potential pathogen identification, the high-quality sequences were blasted against the reference database of bacterial pathogen 16S rRNA sequences, as described by our previous study with an *E*-value < 1×10^{-5}.[32] The best hit outputs were then filtered with a strict similarity threshold (>99%) and annotated by taxonomic identity. All sequencing data have been deposited in the National Center for Biotechnology Information (NCBI) Sequence Read Archive (SRA) under the accession number SRP269246.

https://dx.doi.org/10.1021/acs.est.0c04292
Environ. Sci. Technol. 2020, 54, 11322−11332

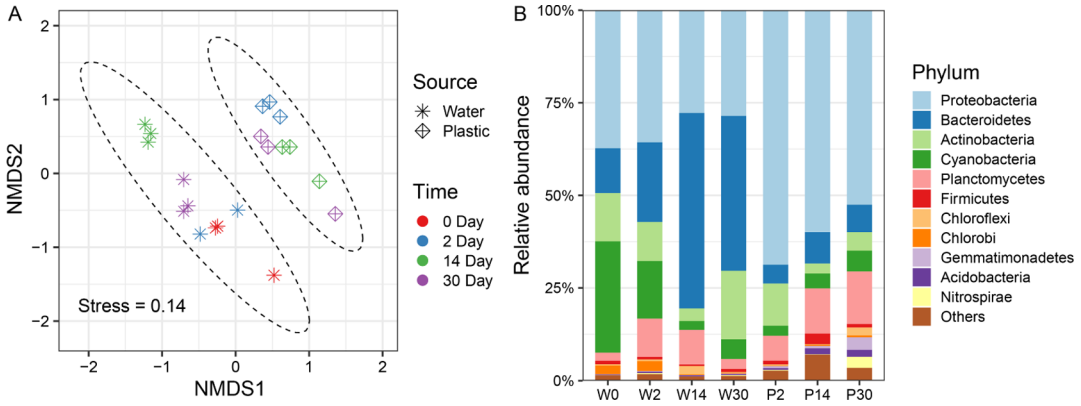

Figure 2. Taxonomic profiles of microbial communities in the plastisphere and the surrounding water during colonization. (A) NMDS based on Bray−Curtis distances showing the patterns of microbial communities (ANOSIM, $R = 0.638$, $P = 0.001$). (B) Relative abundance of bacterial phyla present in the plastisphere and the surrounding water during colonization at days 0, 2, 14, and 30. P: plastisphere; W: surrounding water.

D_2O-Labeled Single-Cell Raman Spectroscopy. Single-cell Raman spectroscopy combined with D_2O labeling was performed according to our previous studies with modifications.[33] Briefly, plastic samples with surrounding water were collected after 30 days of incubation. One volume of the water sample was mixed with one volume of D_2O in a six-well plate, producing a final concentration of 50% (v/v) D_2O. The water was then amended with a proper amount of ciprofloxacin (CIP) to reach final concentrations of 0, 1, and 10 μg mL^{-1}, respectively. Plastic samples were immersed in water and incubated at room temperature on a microplate shaker at 300 rpm for 24 h. Thereafter, microbes on plastic samples were detached by vigorously vortexing for 5 min in 5 mL PBS supplemented with 0.5% (v/v) Tween 20 (Aladdin). After centrifugation and washing with sterile water, 2 μL of microbes from plastisphere and free-living microbes in water were spotted on an aluminum (Al) foil substrate and dried at room temperature prior to single-cell Raman spectral acquisition. Single-cell Raman spectroscopy was performed using a LabRAM Aramis (HORIBA Jobin-Yvon, Japan) confocal micro-Raman system equipped with a 532 nm Nd:YAG excitation laser and a 300 grooves/mm diffraction grating. A 100× dry objective (N.A. = 0.9, Olympus, Japan) was employed for bacterial observation and spectral acquisition. The spectra were processed by baseline correction and normalization in LabSpec 5 (HORIBA Jobin-Yvon, Japan) software. The bands assigned to CD (2040−2300 cm^{-1}) and CH (2800−3100 cm^{-1}) were integrated to calculate the ratio of CD/(CD + CH) to indicate the deuterium incorporation extent.

Statistical Analysis. All statistical analyses on the raw data were performed in R (3.5.3 version).[34] Averages and standard deviations were calculated using the "plyr" package with customized scripts.[35] One-way analysis of variance (ANOVA) with Tukey's multiple comparison test was conducted in GraphPad Prism 5 for significance analysis; $P < 0.05$ was considered significant. Nonmetric multidimensional scaling (NMDS) based on Bray−Curtis distances, analysis of similarities (ANOSIM) test, Mantel tests based on Spearman correlation, and Procrustes analysis was performed using the "vegan" package.[36] Gephi (0.9.2 version) software was used to visualize the bipartite network graphs.

RESULTS

Physicochemical Properties of Microbial Colonization on Plastic Surfaces. After the initial 2 days of incubation, a submonolayer of microbes of different shapes (cocci and rods) was clearly observed to colonize on the plastic surface (Figure 1A,B). Interestingly, numerous microbial filamentous appendages projecting outward from microbes were observed to anchor to plastics, promoting the stable attachment of pioneering microbes onto plastics (Figure 1A). When the incubation time was increased to 14 days, more microbes attached and clumped onto the plastic surfaces to form tiny and patchy microbial clusters (Figure 1C,D). No clear individual cells can be observed, indicating that EPS secreted by microbes enabled microbes and suspended particles in water to clump together. After 30 days of incubation, large microbial clusters were frequently observed and their thickness reached about 15 μm, as observed in the cross-sectional view of the SEM image (Figure 1E), indicating the formation of thick and multilayer biofilms on plastics. In addition, a quantitative biofilm assay showed that the biomass of the biofilm on the plastic surface increased significantly during the incubation, especially from 14 to 30 days (Figure 1G, $P < 0.001$), consistent with the SEM observations. Along with biofilm formation, plastic surfaces were found to become less hydrophobic with the contact angle decreasing from 90.58 to 55.41° at 10 s successions (Figure 1H). Concomitantly, qualitative assessment of plastic buoyancy showed that plastics moved from floating at the water−air interface to finally sinking into water with time (Figure S1).

Microbial Community Composition in the Plastisphere during Colonization. A total of 9,641,893 high-quality sequences were obtained from plastics and water samples, with sequences per sample ranging from 27,978 to 367,408. Overall, 8288 representative amplicon sequence variants (ASVs) were generated after taxonomic assignment. Rarefaction curves of ASVs at the sequencing depth of 20,666 from different sampling times in plastisphere and water are shown in Figure S2. During the colonization process, both the microbial community in the plastisphere and the surrounding water varied with time. Moreover, the pattern of microbial community in the plastisphere in all four sampling times deviated significantly from that of the surrounding water (ANOSIM, $R = 0.638$, $P = 0.001$, 999 permutations) (Figure 2A).

https://dx.doi.org/10.1021/acs.est.0c04292
Environ. Sci. Technol. 2020, 54, 11322−11332

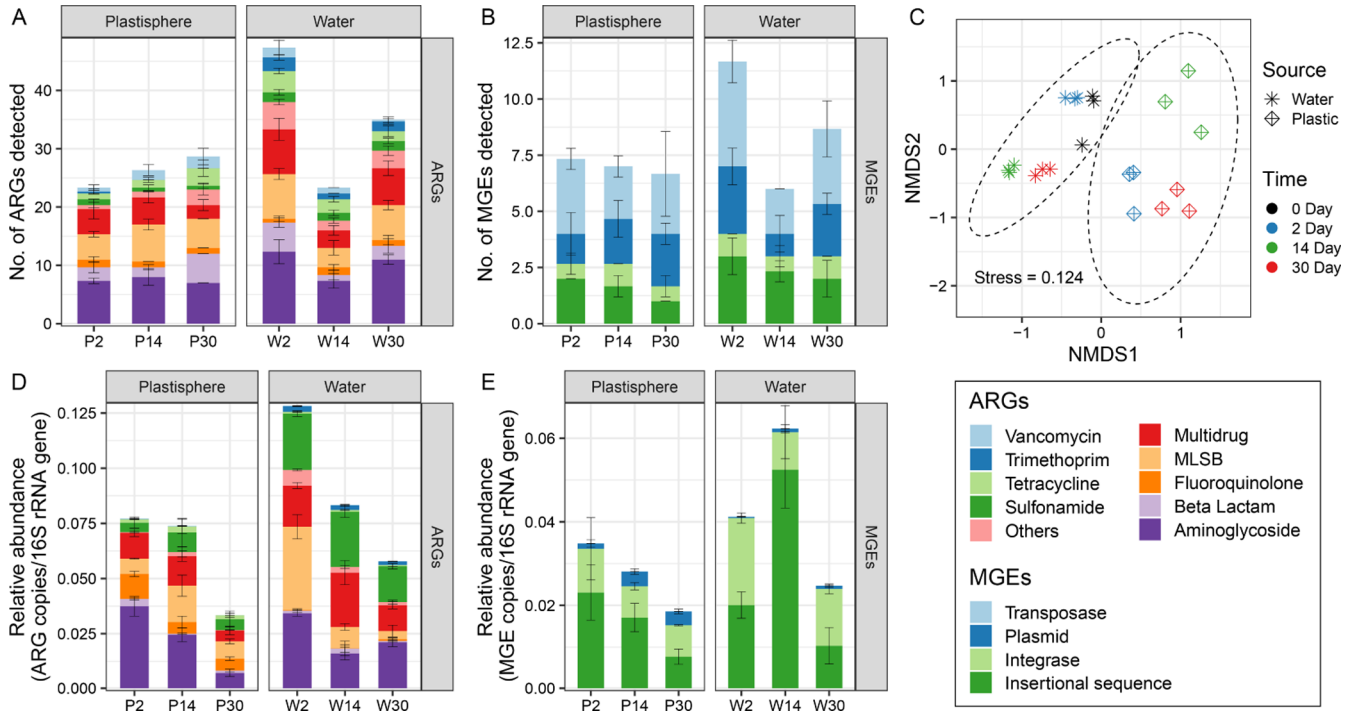

Figure 3. Resistome profiles of the plastisphere and the surrounding water. Detected number of ARGs (A) and MGEs (B) in the plastisphere and the surrounding water at days 2, 14, and 30. (C) NMDS analysis of resistome based on Bray−Curtis distances in plastisphere and water (ANOSIM, $R = 0.7293$, $P = 0.001$). Relative abundance of ARGs (D) and MGEs (E) in the plastisphere and the surrounding water at days 2, 14, and 30. P: plastisphere; W: surrounding water.

After 2 days of incubation, the pioneering microbes initially colonized on the plastic surfaces were dominated by *Proteobacteria* (68.73%), *Actinobacteria* (11.4%), *Planctomycetes* (6.71%), *Bacteroidetes* (5.05%), *Cyanobacteria* (2.68%), and *Firmicutes* (1.03%) (Figure 2B). By comparison, the source water was dominated by *Proteobacteria* (35.67%), *Bacteroidetes* (21.5%), *Cyanobacteria* (15.56%), *Actinobacteria* (10.55%), *Planctomycetes* (10.33%), and *Chlorobi* (2.68%) (Figure 2B). During the following colonization process on plastics, the Shannon index indicated that the bacterial alpha-diversity in the plastisphere increased significantly (Table S2, ANOVA, $P < 0.05$). The abundance of *Proteobacteria* decreased but still maintained the highest value ranging from 59.93 to 52.52% on the plastic surface at days 14 and 30, respectively. The abundance of *Actinobacteria* (5%) at day 30 dropped to less than half of abundance at day 2. In contrast, the relative abundance of *Planctomycetes*, *Cyanobacteria*, *Gemmatimonadetes*, and *Acidobacteria* increased on the plastic surface during the 30-day colonization process.

Occurrence of Potential Bacterial Pathogens in the Plastisphere. Approximately, 0.85% of all high-quality sequences were identified to be potential pathogens affiliated with 76 bacterial pathogenic species. The top 20 abundant species in all samples are shown in Figure S3. In the plastisphere, the top two dominant bacterial pathogens were *Mycobacterium abscessus* (35.07%) and *Bacillus megaterium* (23.63%), followed by *Mycobacterium gilvum* (9.9%), *Listeria monocytogenes* (7.74%), and *Pseudomonas putida* (7.58%). Different from plastisphere, the top two dominant bacterial pathogens in the surrounding water were *L. monocytogenes* (29.49%) and *M. abscessus* (14.72%), followed by *Pseudomonas mendocina* (8.56%), *M. gilvum* (8.05%), *B. megaterium* (7.38%), and *P. putida* (7.37%). Among these species, the relative abundance of *M. abscessus*, *B. megaterium*, and *M. gilvum* in the plastisphere was significantly higher (*t*-test, $P < 0.01$) than that in the surrounding water. Moreover, the ratio of pathogens to total bacteria in the plastisphere was significantly higher (*t*-test, $P < 0.05$) than that in all water samples. These findings suggest a potentially higher health risk of plastisphere than the water body.

Temporal Dynamics of Antibiotic Resistome in the Plastisphere during Colonization. A total of 94 genes were detected in the plastisphere, including 82 ARGs and 12 MGEs (Figure 3A,B). This number was less than that in water with a total of 148 genes including 120 ARGs and 28 MGEs (Figure 3A,B), indicating that the diversity of both ARGs and MGEs in the plastisphere was generally lower than that in water. These detected ARGs conferred resistance to nine major classes of antibiotics commonly administered to humans and animals, including aminoglycosides, β-lactams, fluoroquinolones, multidrugs, macrolide-lincosamide-streptogramin B (MLSB), sulfonamides, tetracycline, trimethoprim, and vancomycin (Figure S4). Moreover, a total of 18 genes including 12 ARGs and 6 MGEs were shared between plastisphere and water, and the major ARGs contributors were aminoglycoside, fluoroquinolone, MLSB, multidrug, sulfonamide, and tetracycline resistance genes (Figure S5).

During microbial community colonization on plastics, the resistome profile in the plastisphere differed significantly from that in water across all sampling times (Figure 3C, ANOSIM, $R = 0.7293$, $P = 0.001$, 999 permutations). Notably, the detected number of ARGs in the plastisphere was found to increase remarkably with time (Figure 3A, ANOVA, $P < 0.05$), while that of MGEs was relatively stable (Figure 3B). In addition, despite the rapid increase of biomass in the plastisphere (Figure 1G), the relative abundance of ARGs

https://dx.doi.org/10.1021/acs.est.0c04292
Environ. Sci. Technol. 2020, 54, 11322−11332

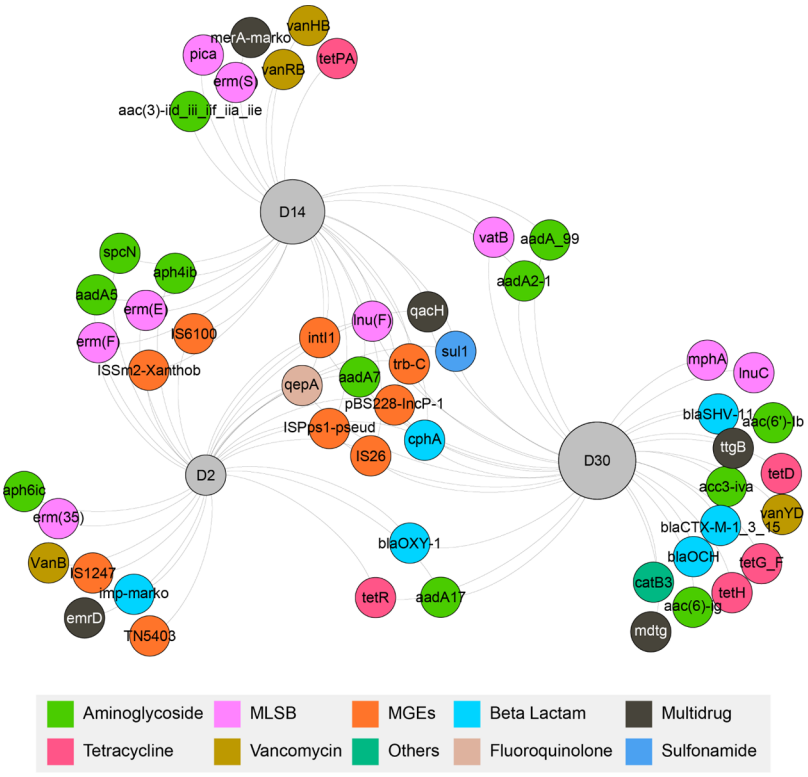

Figure 4. Shared resistome in the plastisphere during microbial colonization at days 2, 14, and 30. Representative resistome was selected from the plastisphere (ARG subtypes that occurred in at least 67% of the total samples) to generate the network.

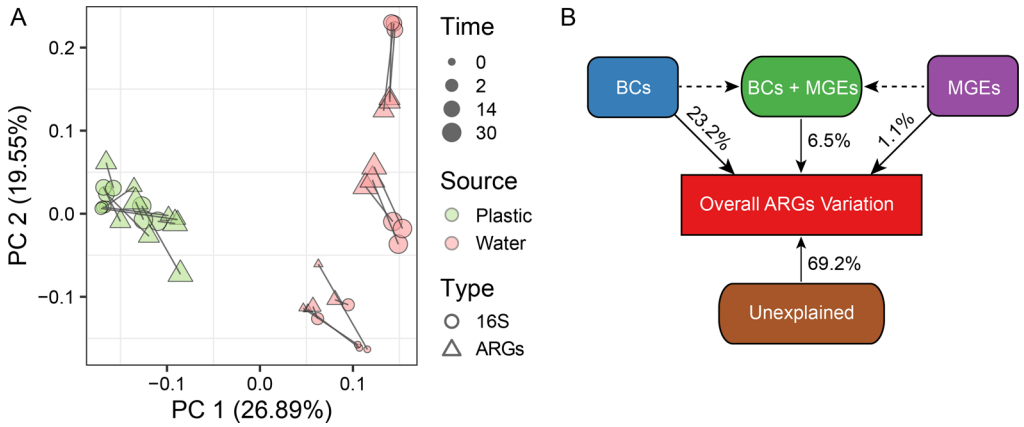

Figure 5. Correlation between the resistome and microbial communities. (A) Procrustes analysis depicting the significant correlation between the resistome and the bacterial composition on the basis of Bray−Curtis dissimilarity metrics (sum of squares $M^2 = 0.3013$, $r = 0.8359$, $P < 0.0001$, and 9999 permutations). (B) VPA differentiating the effect of BCs and MGEs on resistome alteration.

and MGEs in the plastisphere decreased with time (Figure 3D,E).

To better illustrate the temporal variation of antibiotic resistome in the plastisphere, a bipartite association network was used to analyze the shared resistome during microbial colonization (Figure 4). The temporal dynamics of the resistome patterns were categorized into four different categories with the third one being of major concern. They are described by time series (Figure 4): (i) 7 pioneering genes including 5 ARGs and 2 MGEs exclusively detected at day 2 but not at day 14 and day 30. These genes just lasted a short time in the plastisphere and thus were of little concern. (ii) 20 intermediate genes (18 ARGs and 2 MGEs) including those exclusively detected at day 14 and those shared between days 2 and 14, 2 and 30, and 14 and 30. They lasted for a relatively long time but only contained two types of MGEs assigned to the insertional sequence, and should be of possible concern; (iii) 11 persistent genes including 6 ARGs and 5 MGEs always detectable in the plastisphere from days 2 to 30. They not only lasted long but contained a high number of MGEs, increasing the spreading risks of ARGs through horizontal gene transfer (HGT), and thus should be of major concern. The shared 6 ARGs conferred resistance to aminoglycosides (*aadA7*), β-lactams (*cphA*), fluoroquinolones (*qepA*), MLSB (*lnu(F)*), multidrugs (*qacH*), and sulfonamides (*sul1*). The shared 5 MGEs (*intI1*, *IS26*, *ISPps1-pseud*, *pBS228-IncP-1*, and *trb-C*) were reported to play important roles in HGT; (iv) 15 genes newly detected at day 30. These genes should come from the

https://dx.doi.org/10.1021/acs.est.0c04292
Environ. Sci. Technol. 2020, 54, 11322−11332

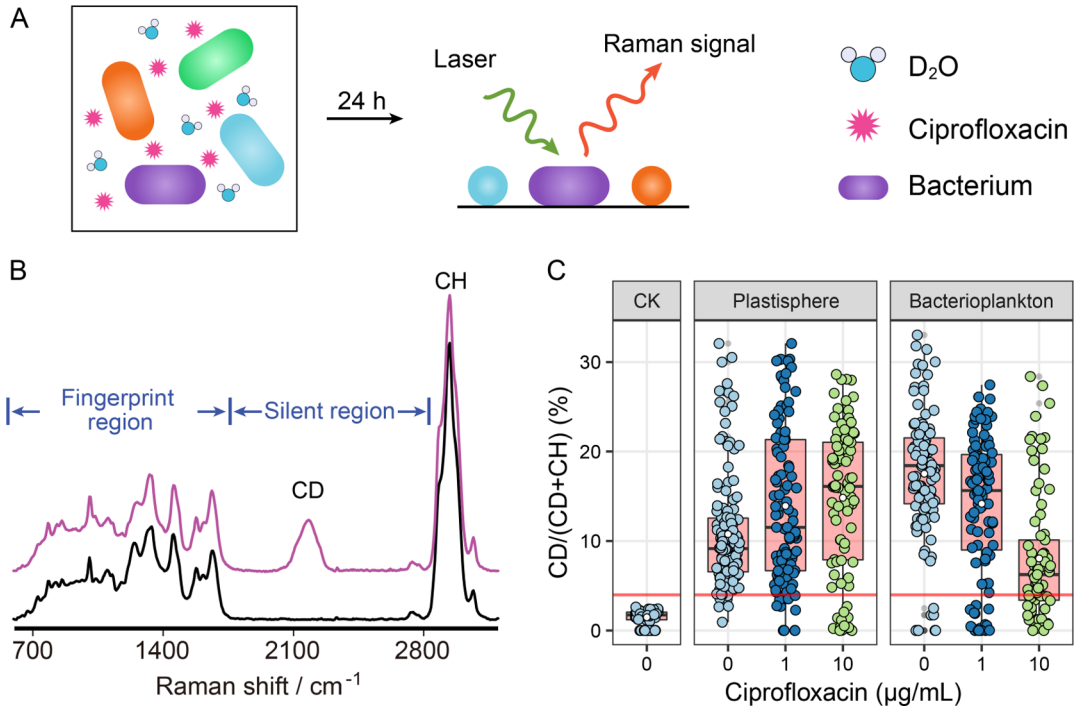

Figure 6. Single-cell Raman spectroscopy combined with heavy water revealing the phenotypic antibiotic tolerance of the plastisphere biofilm and planktonic bacteria under CIP treatment. (A) Schematic representation of the single-cell Raman-D_2O method for assessing bacterial metabolic activity. (B) Typical single-cell Raman spectra of deuterium-labeled and unlabeled bacteria. (C) Distribution quartiles of C−D ratios measured from around 100 randomly selected single cells in the plastisphere or bacterioplankton. Each point is a measurement of one single cell. The red horizontal line at 3.98% C−D ratios shows the threshold for detection. It was defined as the mean + 3 SD of C−D ratios from randomly selected bacteria incubated without heavy water.

increased diversity of microbial species colonized on plastics at day 30.

Correlation between ARGs and Microbial Communities. A Mantel test showed that ARG profiles significantly correlated with BCs based on the Bray−Curtis distance (r = 0.5759, P < 0.0001, 9999 permutations). Procrustes analysis indicated that most of the ARGs' HT-qPCR data and bacterial 16S rRNA gene ASVs of plastisphere or water were well clustered every time during the colonization process by exhibiting a goodness-of-fit test (sum of squares M^2 = 0.3013, r = 0.8359, P < 0.0001, and 9999 permutations) on the basis of Bray−Curtis dissimilarity metrics (Figure 5A). Redundancy analysis was further performed to understand the relationships between BCs, MGEs, and ARGs. The first two axes accounted for 51.08 and 22.7% of the ARG variation in plastic and water samples (Figure S6). Three major phyla, *Cyanobacteria*, *Chlorobi*, and *Spirochaetes*, were all negatively correlated with the first axis. Additionally, all MGEs negatively correlated with the first axis except plasmids. By designating the explanatory variables and covariates, variation partitioning analysis (VPA) separated the influence of BCs and MGEs and showed that the BCs contributed the most (23.2%) to the change of ARGs, followed by the interaction between BCs and MGEs (6.5%), and then MGEs (1.1%) (Figure 5B).

Antibiotic Tolerance of Bacteria Colonized in the Plastisphere. In addition to characterizing the plastisphere at the genomic level, phenotypic antibiotic tolerance of plastisphere was also studied at the physiological level. As most of the bacteria in the environment are yet uncultured,[37] the single-cell technique provides a good means to circumvent the necessity of pure culture and study environmental microorganisms directly. Single-cell Raman spectroscopy is an emerging technique capable of deciphering the phenotypic profile of individual members in a microbial community in a culture-independent way.[38−40] When further combined with D_2O labeling (Raman-D_2O), physiologically active microbes can incorporate deuterium (D) into *de novo*-synthesized lipids and proteins *via* NADH or NADPH electron-transport chain, generating a new carbon−deuterium (C−D) Raman band (Figure 6A,B).[33,40] Interrogation of the C−D band of microbes allows distinguishing the antibiotic-tolerant and sensitive cells because of their different activities under antibiotic treatment. This method has successfully identified antibiotic resistant and sensitive cells in both clinical urine and environmental river.[33,41] Here, single-cell Raman-D_2O was employed to compare the antibiotic tolerance of individual microorganisms colonized in the plastisphere with that of bacterioplankton in water based on their metabolic activities in response to antibiotics.

Considering that fluoroquinolone resistance genes were extensively and persistently detected in nearly all plastic and water samples during the colonization process (Figures 4 and S6), CIP, a proxy of fluoroquinolone and clinically relevant antibiotic, was chosen to investigate the antibiotic tolerance of bacteria in the plastisphere. As shown in Figure 6C, in the absence of CIP, the C−D ratios of free-living bacteria in water were higher than those of bacteria in the plastisphere (ANOVA, P < 0.001), indicating that free-living bacteria were more active than the colonized bacteria on plastics. The reason should be related to the easier access of free-living bacteria to nutrition and oxygen in water than biofilms. However, after exposure to 1 μg mL^{-1} and an escalating dose of 10 μg mL^{-1} CIP, the C−D ratios of free-living bacteria reduced significantly (ANOVA, P < 0.05), indicating that their

https://dx.doi.org/10.1021/acs.est.0c04292
Environ. Sci. Technol. 2020, 54, 11322−11332

metabolic activity was inhibited by CIP. By comparison, the C−D ratios of colonized bacteria in the plastisphere exhibited no significant differences under CIP treatment from control, even at a higher concentration of 10 μg mL^{-1} CIP, indicating that the metabolic activity of colonized bacteria on plastics was not affected by antibiotics. These contrasting behaviors clearly indicated that bacteria in the plastisphere were more tolerant to antibiotics than free-living ones and thus can be more persistent in the environment and induce a higher risk.

DISCUSSION

Temporal Dynamics of Microbial Composition and Antibiotic Resistome in the Plastisphere. The present study provided a comprehensive temporal profile of antibiotic resistome and microbial composition in the plastisphere during microbial colonization on polyethylene plastic debris exposed to an urban water body. Compared with previous studies mainly focusing on field sampling and neglecting the colonization process,[14,15,27] this work presented an in-depth analysis of the temporal dynamics of plastisphere, from the initially few bacteria sparsely colonized on the plastics to forming tiny, patchy, and large microbial clusters with a thickness of around 15 μm.

During the colonization process, both the microbial community in the plastisphere and the surrounding water varied with time. The profile of microbial composition on plastics differed significantly from that in water at all times, suggesting that plastics provide a novel niche selectively harboring microbes from the surrounding water, consistent with previous reports that the microbial community structures associated with the plastic surface were distinct from the surrounding environment.[29,42] This selection process occurred at the early colonization stage of day 2, and the pioneering bacteria were found to strongly bond to the plastic surface by microbial appendages (i.e., fimbriae and pili). These pioneering bacteria were dominated by families of *Comamonadaceae* (48.4%), *Patulibacteraceae* (5.25%), *Pirellulaceae* (2.20%), *Moraxellaceae* (1.9%), *Planctomycetaceae* (1.82%), *Mycobacteriaceae* (1.68%), *Xanthomonadaceae* (1.04%), and *Flavobacteriaceae* (1.01%) (Figure S7). They played an important role in cell adhesion, nutrient metabolism, and element cycling. For instances, *Comamonadaceae* members have been widely found in the early stages of biofilm formation because they can produce EPS to initiate the cell adhesion and facilitate successive colonizers.[43] Species that belonged to *Patulibacteraceae* and *Xanthomonadaceae* were reported to be hydrocarbon degraders,[7,44] suggesting their potential roles in nutrient metabolism and element cycling. Species in the family of *Flavobacteriaceae* were documented as keystone taxa that preyed on diatoms *via* lysis,[45] indicating their potential function in microbial food web in the plastisphere. The diversity of plastisphere increased significantly with time, consistent with the SEM observations and quantitative biofilm assay that more bacteria colonized on plastics. Moreover, the increase of hydrophilicity of plastisphere accompanied by the sinking of plastics from the water−air interface to the waterbody may also affect the microbial community in the following colonization process.

In addition to microbial composition, the detected number of ARGs and MGEs was also found to increase significantly during microbial community assembling in the plastisphere. A total number of 82 ARGs and 12 MGEs were detected in the plastisphere, confirming that plastics can accumulate diverse antibiotic resistome in aquatic environments. This is consistent with previous observations that plastics were reservoirs of ARGs in the marine environment.[14] Intriguingly, the resistome profile in the plastisphere differed significantly from that in water across all sampling times, indicating the selective harboring of antibiotic resistome in the plastisphere. In contrast, the relative abundance of ARGs decreased significantly in the plastisphere during the colonization process. The reason should be related to the significant increase of microbial abundance in the plastisphere, as evidenced by the increase of microbial biomass (Figure 1G) and the Shannon index (Table S2).

A key finding of this study was the recognition of temporal dynamics of resistome together with the identification of pioneering, intermediate, and persistent ARGs and MGEs during the microbial colonization process. Of major concerns were the 5 MGEs and 6 ARGs persistent in the plastisphere during the 30 days of incubation. The high number of MGEs together with the long existence time raised the risk of disseminating ARGs *via* HGT in the plastisphere. Among the MGEs persistently detected in the plastisphere, class 1 integron-integrase genes (*intI1*) were reported to play a key role in the transmission of ARG cassettes among Gram-negative bacteria.[46] Moreover, biofilm conditions were reported to favor integron-mediated acquisition of antibiotic resistance by the bacterial stringent response,[47] indicating their contribution for disseminating ARGs in the plastisphere. In addition, *trb-C* genes were reported to play an important role in the conjugative process mediated by type IV secretion system,[48] potentially facilitating the transconjugation of ARG plasmids into pathogens. Among the persistent ARGs in plastisphere, *cphA* encoded metallo-β-lactamase resistance to the last-resort carbapenem antibiotics,[49] emphasizing its potential risks in aquatic ecosystems.

Potential Risk of Plastisphere to Aquatic Ecosystems and Human Health. The risks of plastisphere can be recognized from four aspects, that is, pathogens harbored in the plastisphere, potential acquisition of ARGs though HGT, increased tolerance to antibiotics, and trophic transfer *via* the food web. In our work, a total of 63 bacterial pathogens related to human diseases were identified in the plastisphere, and the ratio of pathogens to total bacteria in the plastisphere was significantly higher than that in water, suggesting a potentially higher health risk of plastisphere than water. Moreover, 12 MGEs including integrase and transposase genes were detected in the plastisphere. Considering the aggregated microbial cluster on plastics, plastisphere provides an ideal space for pathogens to acquire resistance *via* HGT, which could be further accelerated by the adsorbed organic and inorganic chemicals on plastics.

Furthermore, microbes in the plastisphere were demonstrated to be more antibiotic-tolerant than free-living bacteria, as revealed by the single-cell Raman-D_2O method at the physiological level. In a biofilm structure, microbial consortia were embedded in the self-secreted EPS consisting of polysaccharide, protein, and DNA.[30] Therefore, the plastisphere mode-of-growth provides a shelter for bacteria to mitigate antibiotic invasion. This not only enables antibiotic resistance to persist in the plastisphere for a long time but also buys time for the adaptive antibiotic genetic changes through HGT or mutation, thereby posing a long-term environmental risk. These observations also underline the importance of phenotypic studies of microbes in the plastisphere, which have

https://dx.doi.org/10.1021/acs.est.0c04292
Environ. Sci. Technol. 2020, 54, 11322−11332

profound ecology implications, especially in heavily polluted environments.

Some studies demonstrated that organisms, such as turtles, fish, mammals, and invertebrates can uptake plastic debris into the intestinal tract *via* mistaken ingestion or food web in aquatic environments.[25,26] Some recent studies further revealed that ARGs can transfer through the trophic level into the food chain.[50] As such, the ARGs harbored on plastics could potentially enter the food chain *via* aquatic food products, posing negative effects on aquatic ecosystems and even human health. More studies are needed to fully elucidate the transfer pathway of ARGs in the plastisphere from aquatic food products to humans.

In summary, this study revealed the dynamics of antibiotic resistome and microbial community on plastics from the initial microbial colonization to biofilm development in an urban waterbody. The pioneering, intermediate, and especially a high number of persistent MGEs and ARGs in the plastisphere were identified, indicating the great role of plastisphere in disseminating antibiotic resistance. Furthermore, single-cell physiological analysis *via* Raman-D_2O revealed that plastisphere was more antibiotic tolerant than free-living bacteria. Finally, an integrated analysis of the potential risks of plastisphere was performed at both genomic and physiological levels. The persistence of MGEs, enriched colonization of pathogenic bacteria, increased antibiotic tolerance, and the potential trophic transfer indicated that plastisphere was a hot spot for acquiring and spreading antibiotic resistance and disease and may have a long-term negative effect on the ecosystem and the human health. Together, these findings provide important insights into the development of antibiotic resistome in the plastisphere. Considering that plastics can persist for a long time in the environment and plastisphere provides a shelter for antibiotic resistance to persist and even evolve *via* HGT or mutation, in the future, it is necessary to perform a long-term study to evaluate the ecological and health risks of the plastisphere.

■ ASSOCIATED CONTENT

Supporting Information

The Supporting Information is available free of charge at https://pubs.acs.org/doi/10.1021/acs.est.0c04292.

Experimental description of biofilm quantification in the plastisphere; additional details on library preparation and sequence data processing; basic parameters of source water; list of primers used in this study; buoyancy test of plastic samples; rarefaction curves of sequences; relative abundance of bacterial pathogens in water and plastisphere; ARG profiles in water and plastisphere; microbial composition of water and plastisphere; and picture of the biofilm reactor used in this study (PDF)

■ AUTHOR INFORMATION

Corresponding Author

Li Cui − *Key Laboratory of Urban Environment and Health, Institute of Urban Environment, Chinese Academy of Sciences, Xiamen 361021, China;* orcid.org/0000-0002-0708-8899; Phone: 86-5926190560; Email: lcui@iue.ac.cn

Authors

Kai Yang − *Key Laboratory of Urban Environment and Health, Institute of Urban Environment, Chinese Academy of Sciences, Xiamen 361021, China; University of Chinese Academy of Sciences, Beijing 100049, China;* orcid.org/0000-0002-3554-3334

Qing-Lin Chen − *Faculty of Veterinary and Agricultural Sciences, The University of Melbourne, Parkville, Victoria 3010, Australia*

Mo-Lian Chen − *Key Laboratory of Urban Environment and Health, Institute of Urban Environment, Chinese Academy of Sciences, Xiamen 361021, China; University of Chinese Academy of Sciences, Beijing 100049, China;* orcid.org/0000-0001-8057-9910

Hong-Zhe Li − *Key Laboratory of Urban Environment and Health, Institute of Urban Environment, Chinese Academy of Sciences, Xiamen 361021, China; University of Chinese Academy of Sciences, Beijing 100049, China*

Hu Liao − *Key Laboratory of Urban Environment and Health, Institute of Urban Environment, Chinese Academy of Sciences, Xiamen 361021, China; University of Chinese Academy of Sciences, Beijing 100049, China*

Qiang Pu − *Key Laboratory of Urban Environment and Health, Institute of Urban Environment, Chinese Academy of Sciences, Xiamen 361021, China; University of Chinese Academy of Sciences, Beijing 100049, China*

Yong-Guan Zhu − *Key Laboratory of Urban Environment and Health, Institute of Urban Environment and State Key Laboratory of Urban and Regional Ecology, Research Center for Eco-Environmental Sciences, Chinese Academy of Sciences, Xiamen 361021, China;* orcid.org/0000-0003-3861-8482

Complete contact information is available at: https://pubs.acs.org/10.1021/acs.est.0c04292

Notes

The authors declare no competing financial interest.

■ ACKNOWLEDGMENTS

This work was supported by the National Natural Science Foundation of China (21922608, 21777154), Chinese Academy of Sciences (ZDBS-LY-DQC027), and Key Collaborative Research Program of the Alliance of International Science Organization (ANSO-CR-KP-2020-03).

■ REFERENCES

(1) Geyer, R.; Jambeck, J. R.; Law, K. L. Production, use, and fate of all plastics ever made. *Sci. Adv.* **2017**, *3*, No. e1700782.

(2) Thompson, R. C.; Olsen, Y.; Mitchell, R. P.; Davis, A.; Rowland, S. J.; John, A. W. G.; McGonigle, D.; Russell, A. E. Lost at Sea: Where Is All the Plastic? *Science* **2004**, *304*, 838.

(3) McCormick, A.; Hoellein, T. J.; Mason, S. A.; Schluep, J.; Kelly, J. J. Microplastic is an Abundant and Distinct Microbial Habitat in an Urban River. *Environ. Sci. Technol.* **2014**, *48*, 11863−11871.

(4) Carpenter, E. J.; Anderson, S. J.; Harvey, G. R.; Miklas, H. P.; Peck, B. B. Polystyrene Spherules in Coastal Waters. *Science* **1972**, *178*, 749−750.

(5) Su, L.; Xue, Y.; Li, L.; Yang, D.; Kolandhasamy, P.; Li, D.; Shi, H. Microplastics in Taihu Lake, China. *Environ. Pollut.* **2016**, *216*, 711−719.

(6) Zhang, K.; Xiong, X.; Hu, H.; Wu, C.; Bi, Y.; Wu, Y.; Zhou, B.; Lam, P. K. S.; Liu, J. Occurrence and Characteristics of Microplastic Pollution in Xiangxi Bay of Three Gorges Reservoir, China. *Environ. Sci. Technol.* **2017**, *51*, 3794−3801.

(7) Amaral-Zettler, L. A.; Zettler, E. R.; Mincer, T. J. Ecology of the plastisphere. *Nat. Rev. Microbiol.* **2020**, *18*, 139−151.

(8) Zettler, E. R.; Mincer, T. J.; Amaral-Zettler, L. A. Life in the "plastisphere": microbial communities on plastic marine debris. *Environ. Sci. Technol.* **2013**, *47*, 7137−7146.
(9) Morét-Ferguson, S.; Law, K. L.; Proskurowski, G.; Murphy, E. K.; Peacock, E. E.; Reddy, C. M. The size, mass, and composition of plastic debris in the western North Atlantic Ocean. *Mar. Pollut. Bull.* **2010**, *60*, 1873−1878.
(10) Lamb, J. B.; Willis, B. L.; Fiorenza, E. A.; Couch, C. S.; Howard, R.; Rader, D. N.; True, J. D.; Kelly, L. A.; Ahmad, A.; Jompa, J.; Harvell, C. D. Plastic waste associated with disease on coral reefs. *Science* **2018**, *359*, 460−462.
(11) Ouyang, W.-Y.; Huang, F.-Y.; Zhao, Y.; Li, H.; Su, J.-Q. Increased levels of antibiotic resistance in urban stream of Jiulongjiang River, China. *Appl. Microbiol. Biotechnol.* **2015**, *99*, 5697−5707.
(12) Walsh, C. Molecular mechanisms that confer antibacterial drug resistance. *Nature* **2000**, *406*, 775−781.
(13) Cózar, A.; Echevarría, F.; González-Gordillo, J. I.; Irigoien, X.; Úbeda, B.; Hernández-León, S.; Palma, A. T.; Navarro, S.; García-de-Lomas, J.; Ruiz, A.; Fernández-de-Puelles, M. L.; Duarte, C. M. Plastic debris in the open ocean. *Proc. Natl. Acad. Sci. U.S.A.* **2014**, *111*, 10239−10244.
(14) Yang, Y.; Liu, G.; Song, W.; Ye, C.; Lin, H.; Li, Z.; Liu, W. Plastics in the marine environment are reservoirs for antibiotic and metal resistance genes. *Environ. Int.* **2019**, *123*, 79−86.
(15) Moore, R. E.; Millar, B. C.; Moore, J. E. Antimicrobial resistance (AMR) and marine plastics: Can food packaging litter act as a dispersal mechanism for AMR in oceanic environments? *Mar. Pollut. Bull.* **2020**, *150*, 110702.
(16) Li, J.; Zhang, K.; Zhang, H. Adsorption of antibiotics on microplastics. *Environ. Pollut.* **2018**, *237*, 460−467.
(17) Ashton, K.; Holmes, L.; Turner, A. Association of metals with plastic production pellets in the marine environment. *Mar. Pollut. Bull.* **2010**, *60*, 2050−2055.
(18) León, V. M.; García, I.; González, E.; Samper, R.; Fernández-González, V.; Muniategui-Lorenzo, S. Potential transfer of organic pollutants from littoral plastics debris to the marine environment. *Environ. Pollut.* **2018**, *236*, 442−453.
(19) Teuten, E. L.; Rowland, S. J.; Galloway, T. S.; Thompson, R. C. Potential for Plastics to Transport Hydrophobic Contaminants. *Environ. Sci. Technol.* **2007**, *41*, 7759−7764.
(20) Rios, L. M.; Moore, C.; Jones, P. R. Persistent organic pollutants carried by synthetic polymers in the ocean environment. *Mar. Pollut. Bull.* **2007**, *54*, 1230−1237.
(21) Ye, J.; Rensing, C.; Su, J.; Zhu, Y.-G. From chemical mixtures to antibiotic resistance. *J. Environ. Sci.* **2017**, *62*, 138−144.
(22) Imran, M.; Das, K. R.; Naik, M. M. Co-selection of multi-antibiotic resistance in bacterial pathogens in metal and microplastic contaminated environments: An emerging health threat. *Chemosphere* **2019**, *215*, 846−857.
(23) Parthasarathy, A.; Tyler, A. C.; Hoffman, M. J.; Savka, M. A.; Hudson, A. O. Is Plastic Pollution in Aquatic and Terrestrial Environments a Driver for the Transmission of Pathogens and the Evolution of Antibiotic Resistance? *Environ. Sci. Technol.* **2019**, *53*, 1744−1745.
(24) Arias-Andres, M.; Klümper, U.; Rojas-Jimenez, K.; Grossart, H.-P. Microplastic pollution increases gene exchange in aquatic ecosystems. *Environ. Pollut.* **2018**, *237*, 253−261.
(25) Derraik, J. G. B. The pollution of the marine environment by plastic debris: a review. *Mar. Pollut. Bull.* **2002**, *44*, 842−852.
(26) Seltenrich, N. New Link in the Food Chain? Marine Plastic Pollution and Seafood Safety. *Environ. Health Perspect.* **2015**, *123*, A34−A41.
(27) Lu, J.; Zhang, Y.; Wu, J.; Luo, Y. Effects of microplastics on distribution of antibiotic resistance genes in recirculating aquaculture system. *Ecotoxicol. Environ. Saf.* **2019**, *184*, 109631.
(28) Zhang, Y.; Lu, J.; Wu, J.; Wang, J.; Luo, Y. Potential risks of microplastics combined with superbugs: Enrichment of antibiotic resistant bacteria on the surface of microplastics in mariculture system. *Ecotoxicol. Environ. Saf.* **2020**, *187*, 109852.
(29) De Tender, C.; Devriese, L. I.; Haegeman, A.; Maes, S.; Vangeyte, J.; Cattrijsse, A.; Dawyndt, P.; Ruttink, T. Temporal Dynamics of Bacterial and Fungal Colonization on Plastic Debris in the North Sea. *Environ. Sci. Technol.* **2017**, *51*, 7350−7360.
(30) Flemming, H.-C.; Wingender, J.; Szewzyk, U.; Steinberg, P.; Rice, S. A.; Kjelleberg, S. Biofilms: an emergent form of bacterial life. *Nat. Rev. Microbiol.* **2016**, *14*, 563.
(31) Turner, S.; Pryer, K. M.; Miao, V. P. W.; Palmer, J. D. Investigating Deep Phylogenetic Relationships among Cyanobacteria and Plastids by Small Subunit rRNA Sequence Analysis. *J. Eukaryotic Microbiol.* **1999**, *46*, 327−338.
(32) Chen, Q.; An, X.; Li, H.; Su, J.; Ma, Y.; Zhu, Y.-G. Long-term field application of sewage sludge increases the abundance of antibiotic resistance genes in soil. *Environ. Int.* **2016**, *92*−*93*, 1−10.
(33) Yang, K.; Li, H.-Z.; Zhu, X.; Su, J.-Q.; Ren, B.; Zhu, Y.-G.; Cui, L. Rapid Antibiotic Susceptibility Testing of Pathogenic Bacteria Using Heavy-Water-Labeled Single-Cell Raman Spectroscopy in Clinical Samples. *Anal. Chem.* **2019**, *91*, 6296−6303.
(34) R Core Team. *R: A Language and Environment for Statistical Computing*; R Foundation for Statistical Computing, 2017.
(35) Wickham, H. The Split-Apply-Combine Strategy for Data Analysis. *J. Stat. Software* **2011**, *40*, 29.
(36) Jari, O.; Guillaume, B.; Michael, F.; Roeland, K.; Pierre, L.; Dan, M.; Peter, R. M.; O'Hara, R. B.; Gavin, L. S.; Peter, S.; Henry, H. S.; Eduard, S.; Helene, W. *Vegan: Community Ecology Package*, 2019.
(37) Amann, R. I.; Ludwig, W.; Schleifer, K. H. Phylogenetic identification and in situ detection of individual microbial cells without cultivation. *Microbiol. Rev.* **1995**, *59*, 143−169.
(38) Wang, Y.; Huang, W. E.; Cui, L.; Wagner, M. Single cell stable isotope probing in microbiology using Raman microspectroscopy. *Curr. Opin. Biotechnol.* **2016**, *41*, 34−42.
(39) Cui, L.; Yang, K.; Li, H.-Z.; Zhang, H.; Su, J.-Q.; Paraskevaidi, M.; Martin, F. L.; Ren, B.; Zhu, Y.-G. Functional Single-Cell Approach to Probing Nitrogen-Fixing Bacteria in Soil Communities by Resonance Raman Spectroscopy with $^{15}N_2$ Labeling. *Anal. Chem.* **2018**, *90*, 5082−5089.
(40) Berry, D.; Mader, E.; Lee, T. K.; Woebken, D.; Wang, Y.; Zhu, D.; Palatinszky, M.; Schintlmeister, A.; Schmid, M. C.; Hanson, B. T.; Shterzer, N.; Mizrahi, I.; Rauch, I.; Decker, T.; Bocklitz, T.; Popp, J.; Gibson, C. M.; Fowler, P. W.; Huang, W. E.; Wagner, M. Tracking heavy water (D_2O) incorporation for identifying and sorting active microbial cells. *Proc. Natl. Acad. Sci. U.S.A.* **2015**, *112*, E194−E203.
(41) Song, Y.; Cui, L.; López, J. Á. S.; Xu, J.; Zhu, Y.-G.; Thompson, I. P.; Huang, W. E. Raman-Deuterium Isotope Probing for in-situ identification of antimicrobial resistant bacteria in Thames River. *Sci. Rep.* **2017**, *7*, 16648.
(42) Li, W.; Zhang, Y.; Wu, N.; Zhao, Z.; Xu, W. a.; Ma, Y.; Niu, Z. Colonization Characteristics of Bacterial Communities on Plastic Debris Influenced by Environmental Factors and Polymer Types in the Haihe Estuary of Bohai Bay, China. *Environ. Sci. Technol.* **2019**, *53*, 10763−10773.
(43) Andersson, S.; Dalhammar, G.; Land, C. J.; Kuttuva Rajarao, G. Characterization of extracellular polymeric substances from denitrifying organism Comamonas denitrificans. *Appl. Microbiol. Biotechnol.* **2009**, *82*, 535−543.
(44) Salgado, R.; Brito, D.; Noronha, J. P.; Almeida, B.; Bronze, M. R.; Oehmen, A.; Carvalho, G.; Barreto Crespo, M. T. Metabolite identification of ibuprofen biodegradation by Patulibacter medicamentivorans under aerobic conditions. *Environ. Technol.* **2020**, *41*, 450−465.
(45) Amin, S. A.; Parker, M. S.; Armbrust, E. V. Interactions between Diatoms and Bacteria. *Microbiol. Mol. Biol. Rev.* **2012**, *76*, 667−684.
(46) An, X.-L.; Chen, Q.-L.; Zhu, D.; Zhu, Y.-G.; Gillings, M. R.; Su, J.-Q. Impact of Wastewater Treatment on the Prevalence of Integrons and the Genetic Diversity of Integron Gene Cassettes. *Appl. Environ. Microbiol.* **2018**, *84*, e02766−17.
(47) Strugeon, E.; Tilloy, V.; Ploy, M.-C.; Da Re, S. The Stringent Response Promotes Antibiotic Resistance Dissemination by Regulat-

https://dx.doi.org/10.1021/acs.est.0c04292
Environ. Sci. Technol. 2020, 54, 11322−11332

ing Integron Integrase Expression in Biofilms. *mBio* **2016**, *7*, e00868−16.
(48) Shala-Lawrence, A.; Bragagnolo, N.; Nowroozi-Dayeni, R.; Kheyson, S.; Audette, G. F. The interaction of TraW and TrbC is required to facilitate conjugation in F-like plasmids. *Biochem. Biophys. Res. Commun.* **2018**, *503*, 2386−2392.
(49) Walsh, T. R.; Toleman, M. A.; Poirel, L.; Nordmann, P. Metallo-β-Lactamases: the Quiet before the Storm? *Clin. Microbiol. Rev.* **2005**, *18*, 306−325.
(50) Zhu, D.; Xiang, Q.; Yang, X.-R.; Ke, X.; O'Connor, P.; Zhu, Y.-G. Trophic Transfer of Antibiotic Resistance Genes in a Soil Detritus Food Chain. *Environ. Sci. Technol.* **2019**, *53*, 7770−7781.

https://dx.doi.org/10.1021/acs.est.0c04292
Environ. Sci. Technol. 2020, 54, 11322−11332